R. GHASEMI*, B. BEIDOKHTI**#, M. FAZEL-NAJAFABADI***

# EFFECT OF DELTA FERRITE ON THE MECHANICAL PROPERTIES OF DISSIMILAR FERRITIC-AUSTENITIC STAINLESS STEEL WELDS

The dissimilar welds of AISI 304 to AISI 430 stainless steel was investigated by using gas tungsten arc welding. Three filler metals including ER309L, ER316L and ER2594 were applied. The weakest region of the welds was the heat affected zone of 430 stainless steel due to the formation of martensite. Also, the wide grain growth zone was observed in this side. The ferrite number for type 309L, 316L and 2594 weld metals was about 15, 32 and 57, respectively. The hardness and tensile strength values of the weld metals were higher than that of the heat affected zones and the base metals. The ferrite presented higher hardness values than the austenite in type 316L and 309L joints; while the hardness of austenite and ferrite was comparable in type 2594 weld metal.

*Keywords:* Stainless steel; Welding; Delta ferrite; Electron microscopy; Austenite

## 1. Introduction

The ferritic stainless steels could be substituted for the austenitic stainless steels due to their special properties such as high strength and corrosion resistance in chloride services. Also, they are usually used in oil, gas, petrochemical, nuclear and power industries [1]. The reduced ductility of ferritic stainless steels after welding limits their application in critical situations [2]. This problem has been related to the existence of coarse grains in the weld metal (WM) and the heat affected zone (HAZ) of fusion welds [3]. Although the austenitic stainless steels show their superiority in these cases, the joint between austenitic and ferritic stainless steels may be inevitable in many instances.

The microstructure of dissimilar stainless steel welds depends on the chemical composition of base metals and filler material, and the welding parameters such as heat input and cooling rate. The effect of heat input on the microstructure and mechanical properties of gas tungsten arc welded 304 stainless steel has been studied by Kumar and Shahi [4]. They have reported that the high heat input deposits showed the large average dendrite length in the weld zone.

The value of $Cr_{eq}/Ni_{eq}$ ratio has a significant effect on the solidification mode [5] and the resulting microstructure [6]. Hsieh et al. [7] found that chromium stabilized the massive delta ferrite ($\delta$) in the microstructure of weld metal during dissimilar stainless steel welding. The formation of massive $\delta$-ferrite could increase the hardness values of WM.

The application of matching filler metals imports poor toughness [8] and corrosion resistance [9] of the ferritic stainless steel welds. The grain coarsening has usually been observed in these welds. On the other hand, the ease of welding and proper mechanical properties could be obtained by the austenitic filler metals [10].

Padilha et al. [11] have claimed that the role of chemical composition on the formation of microstructure constituents (e.g. delta ferrite) is more important than the effect of cooling rate. Although austenite and delta ferrite are usually found in the microstructure of stainless steel welds, martensite could be formed in the austenitic matrix of Fe-Ni [12] and Fe-Ni-C alloys [13] by quenching from high temperatures.

The effect of several alloying elements on the properties of Cr-Ni steel joints has been studied. Taban et al. [14] have found that the ductility of the ferritic stainless steel deposits could be improved by using type 309 filler metals instead of type 316 wires. According to Mohandas et al. [1], the addition of titanium and copper promoted the strength of AISI 430 weld metal. Anderson et al. [15] have shown that Mo was more uniformly distributed in the ferritic welds compared to the austenitic ones. Also, sulfur and phosphorus formed liquid films in the interdendritic and grain boundary regions and facilitated the occurrence of solidification cracking. The weld metals with the primary ferrite could be useful to prevent the formation of solidification cracks. The high solubility of P and S in ferrite had a positive impact on the solidification cracking resistance [16]. In the case

\* ISLAMIC AZAD UNIVERSITY, NAJAFABAD BRANCH, DEPARTMENT OF MATERIALS ENGINEERING, ISFAHAN, IRAN
\*\* FERDOWSI UNIVERSITY OF MASHHAD, MATERIALS AND METALLURGICAL ENGINEERING DEPARTMENT, FACULTY OF ENGINEERING, MASHHAD, IRAN
\*\*\* PAYAME NOOR UNIVERSITY, DEPARTMENT OF MECHANICAL ENGINEERING, TEHRAN, IRAN

\# Corresponding author: beidokhti@um.ac.ir

of HAZ cracking, sulfur is more harmful than phosphorus due to the higher diffusion rate and segregation of sulfur in the heat affected zone [17]. Additionally, researchers have believed [18] that the deleterious effect of phosphorus on solidification cracking is higher than that of sulfur. Brooks [19] found the same results in the investigation on the high Mn austenitic stainless steels. It has been suggested [17] that the formation of MnS could reduce the effect of sulfur on solidification cracking.

Although several researches have been done on the properties of stainless steel welds, the task is more challenging in the case of dissimilar joints due to the different composition and metallurgical characterizations. These joints are used widely in petrochemical and food industries (e.g. storage vessels). The objective of this work is to investigate the effect of chemical composition of the weld metal on the microstructure and mechanical properties of dissimilar stainless steel joints.

## 2. Experimental procedures

In this study, AISI 304 austenitic stainless steel and AISI 430 ferritic stainless steel sheets with 3 mm thickness were used as the base plates. The 2.4 mm filler metals employed in this research were ER309L, ER316L and ER2594. The chemical compositions of the base and filler metals are listed in Table 1. Furthermore, WRC-1992 pseudo-binary diagram [2] was used for analysis of the weld metals. The square butt joints with a root gap of 1.5 mm were made using a single pass gas-tungsten arc welding (GTAW) process. The same welding heat input (about 4.7 kJ/mm) and high purity argon shielding gas (99.999%) was applied for all specimens.

The hardness of different regions of the welds was measured using Vickers microhardness testing at a load of 500 g. For each region, the test was repeated 5 times and the average value was reported as the measured hardness. Also, Vickers microhardness measurements were done on the ferrite and austenite phases at a load of 100 g. Both transverse and longitudinal tensile test were carried out; for each, two sub-sized standard tensile samples were prepared according to ASTM E8 (Fig. 1).

Moreover, the transverse sections were cut across the welds, and afterwards were grounded and polished using different grades of emery papers and finally with diamond paste. Then, the electroetching process in 10% oxalic acid was employed to obtain the metallographic sections for optical microscopy stud-
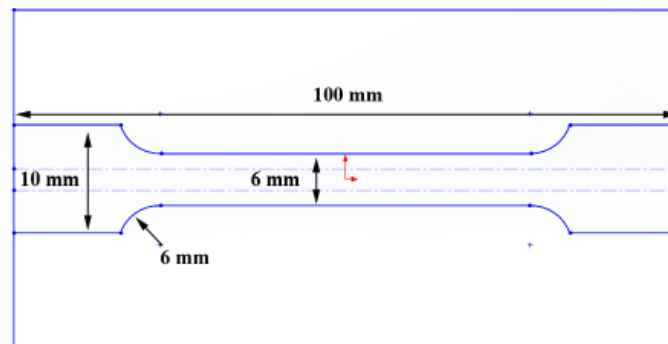


Fig. 1. The schematic illustration of the tensile test samples

ies. The oxalic acid solution could detect probable chromium carbides in the weld area [20]. The characterization of the phases was obtained using a Philips X'pert MPD X-ray diffractometer. The ferrite measurements were performed using an AKA Scan-MP51 ferritoscope. Further studies on the microstructure were done with a Tescan Vega II XMU scanning electron microscope (SEM) linked to a Rontec energy dispersive X-ray spectroscopy (EDS) system.

## 3. Results and discussion

According to Fig. 2(a), the microstructure of 304 stainless steel consisted of austenite ($\gamma$) with small amounts of delta ferrite; while the equiaxed ferrite grains with fine carbide particles were the dominant microstructural phases of 430 stainless steel (Fig. 2(b)).

The same welding conditions produced the same HAZ microstructure in all specimens. According to Fig. 3(a), the HAZ of 304 stainless steel showed a transition zone, and some delta ferrite was observed along the grain boundaries. This ferrite could prevent grain growth and decrease the likelihood of hot cracking. It has been reported that the formation of grain boundary ferrite is encouraged by chromium partitioning towards the solidification boundaries [21] and the increase in $Cr_{eq}/Ni_{eq}$ ratio [22]. Also, the intergranular chromium carbides were found in the HAZ of 304 stainless steel. As shown in Fig. 3(b), the intermittent pits were formed along the grain boundaries after oxalic acid etching due to the removal of chromium carbides.

A mixture of ferrite, martensite and chromium carbide was observed in the HAZ of 430 stainless steel. Martensite was

TABLE 1

The chemical compositions of the base and filler metals

| Composition (wt-%) | C | Si | Mn | P | S | Cr | Mo | Ni | Co | Cu | W | $Cr_{eq}/Ni_{eq}$ * |
|---|---|---|---|---|---|---|---|---|---|---|---|---|
| AISI 304 | 0.07 | 0.5 | 0.9 | 0.030 | 0.010 | 18.3 | 0.27 | 8.2 | 0.1 | 0.1 | 0.02 | 1.78 |
| AISI 430 | 0.18 | 0.4 | 0.4 | 0.020 | 0.006 | 16.1 | 0.03 | 0.1 | 0.02 | 0.1 | 0.02 | 2.90 |
| ER309L | 0.03 | 0.5 | 1.8 | — | — | 23.0 | 0.30 | 13.0 | — | 0.3 | — | 1.60 |
| ER316L | 0.03 | 0.5 | 1.8 | — | — | 19.0 | 2.8 | 11.5 | — | 0.3 | — | 1.67 |
| ER2594 | 0.02 | 0.4 | 0.4 | — | — | 25.0 | 4.0 | 9.8 | — | 0.2 | 0.9 | 2.76 |

*$Cr_{eq}$ = Cr + 1.5 Si + Mo + 2 Ti + 0.5 Nb

$Ni_{eq}$ = Ni + 30 (C + N) + 0.5 Mn + 0.5 Cu + 0.5 Co
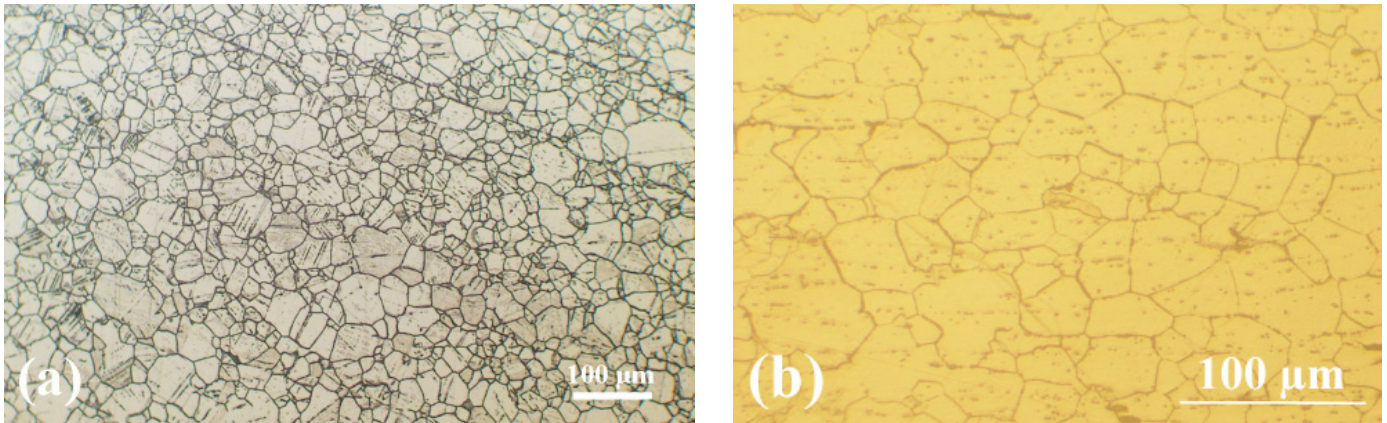
Fig. 2. The microstructure of: (a) AISI 304; (b) AISI 430



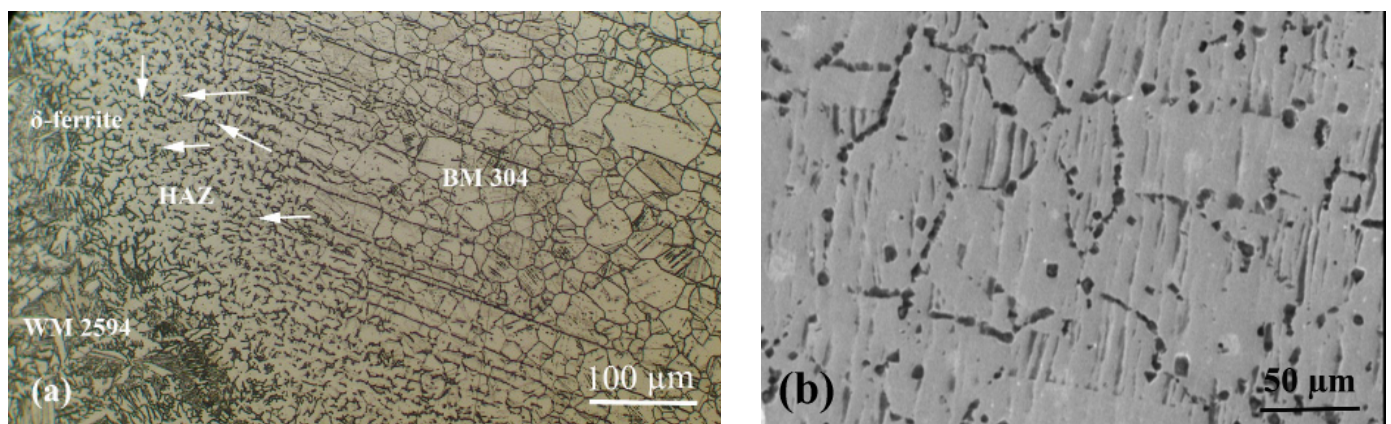Fig. 3. (a) The HAZ of AISI 304 stainless steel adjacent to the WM 2594 (the arrows indicate the formation of δ-ferrite along the grain boundaries); (b) The intermittent pits along the grain boundaries due to pull out of the chromium carbides

found at grain boundaries due to the formation of austenite in the welding thermal cycle as shown in Fig. 4(a). The grain size in the HAZ of type 430 was larger than that in the HAZ of type 304 stainless steel (Fig. 4(b)). It is believed [23] that the driving force for recrystallization is higher in the ferritic steels than in the austenitic ones. Mukherjee and Pal [10] have observed the formation of martensite in ferritic-austenitic dissimilar weldments. They have reported that the formation of martensite promoted the toughness of welds. Contrary to their findings, the mechanical results showed that the formation of martensite and wide grain growth zone in type 430 HAZ imposed deleterious effects on the properties of this region. As shown in Fig. 4(c), an extensive pitting was found in this specimen after oxalic acid etching and confirmed the precipitation of chromium carbide at the grain boundaries. Also, the result of the X-ray diffraction (XRD) pattern could be observed in Fig. 4(d). The less carbon solubility of ferrite compared to austenite could be the cause of more chromium carbide precipitation on cooling.

The microstructure of weld metal depends on the cooling rate and chemical composition of the weld zone. Here, the welding parameters were similar for all specimens. Consequently, the application of diverse filler metals induced different morphologies in the microstructure of weldments. Type 309L weld metal showed the FA solidification mode and the final microstructure

of this specimen was a matrix of austenite with vermicular ferrite (Fig. 5(a)). The value of $Cr_{eq}/Ni_{eq}$ ratio was a little higher for type 316L weldment compared to type 309L joint. As shown in Fig. 5(b), a combination of austenite and acicular ferrite was found in the microstructure of type 316L weld. Increased the $Cr_{eq}/Ni_{eq}$ ratio changed the solidification path from FA to F mode for type 2594 weld metal. In the microstructure of this specimen, Widmanstätten austenite was also largely found in a matrix of ferrite according to Fig. 5(c).

It has been reported that a small amount of delta ferrite in austenite is necessary to prevent hot cracking of stainless steel welds [2]. According to the ferrite measurements, the ferrite number (FN) for type 309L, 316L and 2594 weld metals was about 15, 32 and 57, respectively. Fig. 6 shows the WRC-1992 diagram with the marked actual and expected FN of the welds. The base material dilution was considered 25% by each base metal [24] to calculate the expected ferrite numbers. The maximum amount of ferrite was obtained in the case of ER2594 filler material due to the higher molybdenum and the lower nickel content of this specimen. A juxtaposition of two austenitic welds showed that molybdenum as a ferrite stabilizer element increased the ferrite content in the weld metal of ER316L. Although the existence of ferrite is useful for hot cracking resistance of the weld [25], the excessive amount of ferrite could form a continuous network
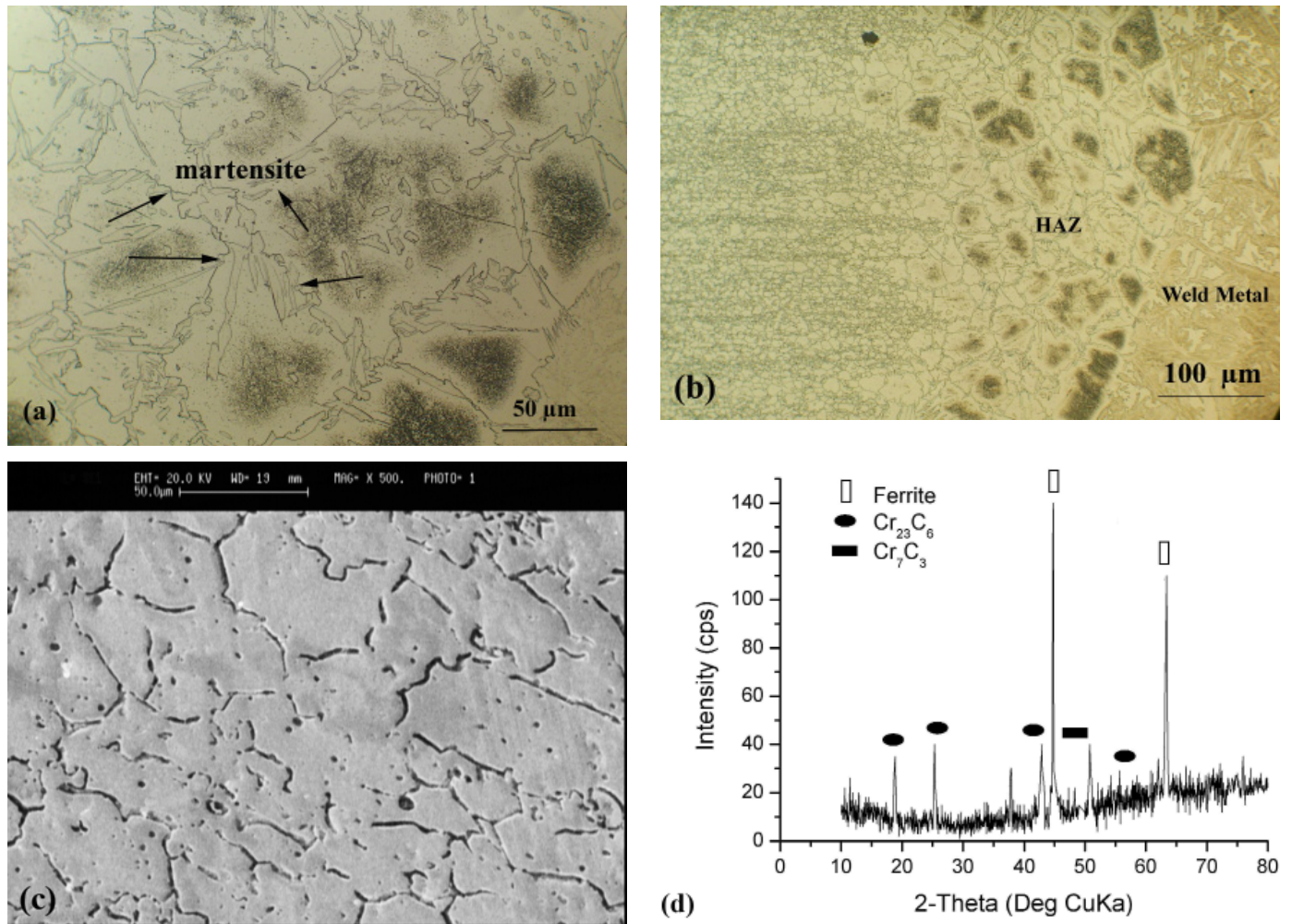
Fig. 4. (a) Formation of martensite at the grain boundaries in the HAZ of AISI 430 stainless steel; (b) Grain growth in this region; (c) The continuous pitting along the grain boundaries due to pull out of the chromium carbides in the HAZ of AISI 430 side; (d) The XRD result of this region

microstructure which would be a favorite site for the nucleation of chromium carbide [26]. The formation of carbide on the austenite-ferrite grain boundaries deteriorates the corrosion and mechanical properties of stainless steel welds.

The hardness profile of different specimens is shown in Fig. 7. It was predicted that the formation of coarse grained region reduced the hardness values in the HAZ of both steels; but the results contradicted this assumption. The precipitation of chromium carbide and the existence of grain boundary delta ferrite in the HAZ of 304 stainless steel caused the increase in hardness. Also, the formation of martensite and chromium carbide hardened the HAZ of 430 base material. The heat affected zone of the ferritic stainless steel had higher hardness values than that of the austenitic one. It seems that the existence of martensite in the ferritic HAZ could be the cause. Vickers microhardness testing revealed that the hardness of martensite was about 425-445 HV, while these values for delta ferrite were in the range of 173-197 HV.

Overall, all weld metals showed higher hardness values than both base materials and heat affected zones. The increased hardness of the WMs could be related to the finer microstructure of the welds, the solid solution hardening and the absence of

chromium-depleted zones (no chromium carbide formation). High cooling rate of the weld metal prevented re-precipitation and grain growth phenomena. Type 316L weld metal showed surprisingly the highest hardness values while the lowest measured hardness belonged to the weld metal of 309L. Repeating the test showed the same results for type 316L weld. First, it seems that the higher percentage of delta ferrite in the weld metal of 316L has increased hardness. On the other hand, the microstructure of type 2594 weldment had the highest percentage of delta ferrite, but the hardness of this weld was not the maximum among the specimens (Fig. 7). For more studies, microhardness measurements were done on the ferrite and austenite phases as given in Table 2. The results showed that the hardness of these phases was comparable in type 2594 weld metal, while delta ferrite presented higher hardness values compared to austenite in type 316L and 309L joints. Ayers [27] showed that the hardness was dependant on the location of hardness testing and the hardness of delta ferrite could be variable along the 316L weld center-line. In conformity with these findings, the hardness values of delta ferrite in the austenitic and duplex welds were different. The elemental analysis of austenite and delta ferrite in the weld metals could be found in Fig. 8. The redistribution of austenite
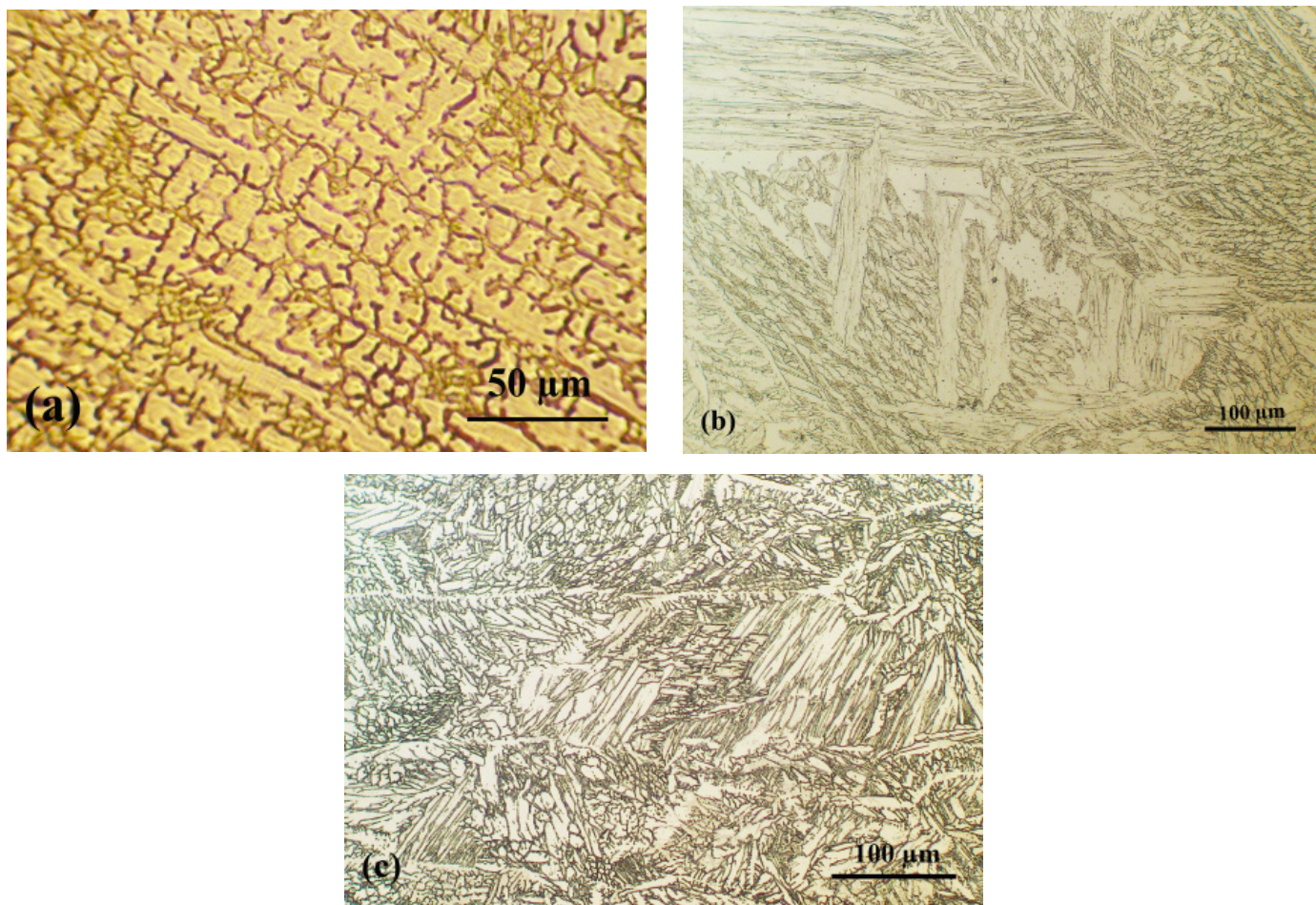
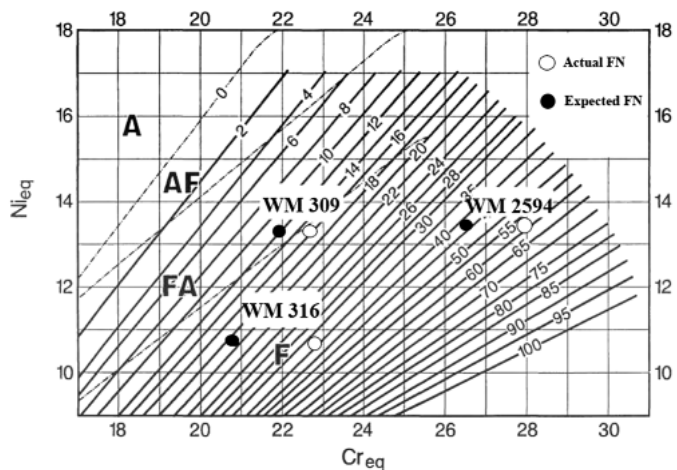Fig. 5. The microstructure of weld metals: (a) 309L; (b) 316L; (c) 2594



Fig. 6. The WRC-1992 diagram showing the actual and expected ferrite numbers
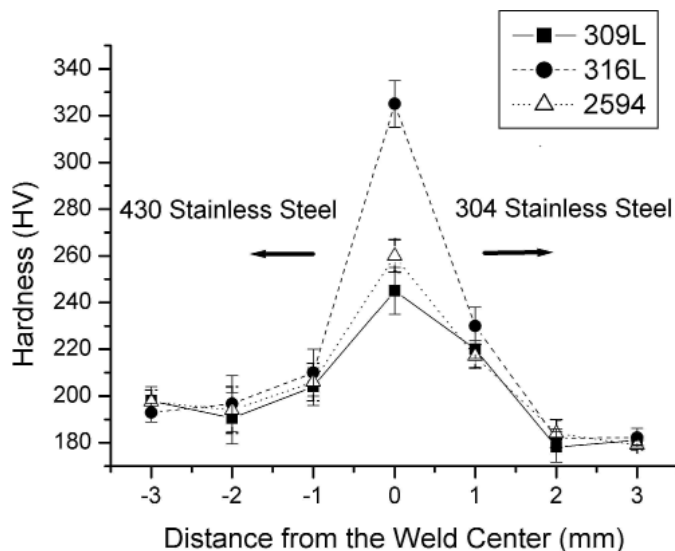


Fig. 7. The hardness profile of each weldment

and ferrite stabilizers was observed in the case of the austenitic filler metals. According to Fig. 8, higher chromium content of delta ferrite in type 316L could be the main cause of the increased hardness value of this specimen. Although the delta ferrite composition was nearly the same in type 309L weldment, it seemed that very low FN value was the dominant factor for decreasing hardness of this joint.

TABLE 2

The microhardness results of different phases in the weld metals

| Weld | Hardness of ferrite (HV) | Hardness of austenite (HV) |
|---|---|---|
| Type 309L | 336 ± 16 | 231 ± 18 |
| Type 316L | 366 ± 17 | 234 ± 20 |
| Type 2594 | 235 ± 10 | 248 ± 14 |

442
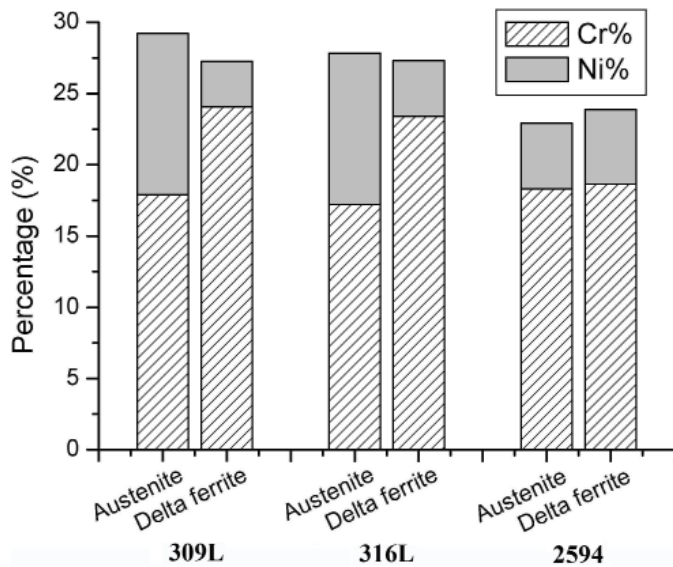


Fig. 8. The elemental analysis of austenite and delta ferrite in the weldments



Fig. 9. The fracture surface in the HAZ of AISI 430 stainless steel

The chemical compositions of delta ferrite and austenite in type 2594 weld metal were similar to each other and led to the same hardness values of these phases. It seems that the dissolution of secondary precipitates during the welding process could redistribute the alloying elements while there is no enough time for re-precipitation on cooling. Furthermore, the same results on the hardness similarity between austenite and ferrite have been reported by other researchers during strain hardening of duplex stainless steels [28]. Although the diffusion of alloying elements is faster in delta ferrite than in austenite [29]; the thermal conductivity of delta ferrite is also higher than that of austenite. Type 2594 weld metal had the highest percentage of delta ferrite and probably the highest cooling rate during welding. Therefore, there was no time for diffusion and redistribution of the austenite and ferrite stabilizers (especially nickel and chromium), and the chemical compositions of austenite and delta ferrite were nearly the same in this weld. However, more studies will be necessary to find the exact mechanisms during welding.

The fracture of all transverse tension samples occurred in the ferritic HAZ. The values of ultimate tensile strength (UTS) for all welds were approximately 409-427 MPa. The HAZ of 430 stainless steel showed the higher hardness values than the ferritic base metal; however the existence of soft delta ferrite adjacent to hard martensite concentrated the deformation in delta ferrite and reduced the strength and ductility of the HAZ. It has been reported [30] that the formation of martensite at grain boundaries of ferrite raised the internal stress and density of mobile dislocations; and then the ferritic microstructure deformed in the stress levels lower than the nominal yield strength of ferrite. Paul [31] found that the strain incompatibility among ferrite and martensite could develop the local stress triaxiality. Despite of the martensite formation in the HAZ of type 430 base metal, the features of brittle fracture were negligible in all specimens. According to Fig. 9, the fracture surfaces exhibited fine dimples indicating the ductile fracture of the specimens.
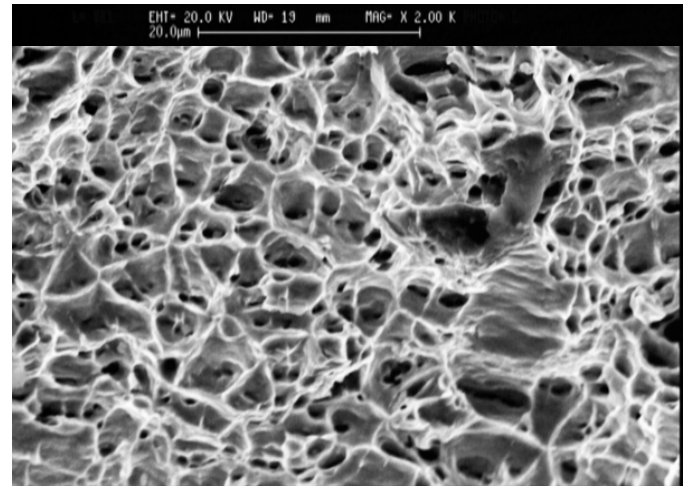
Although the fracture of all transverse tension samples in the HAZ of 430 stainless steel could not provide any information to compare the strengths of different weldments; the results of longitudinal tension tests showed that type 309L weld metal presented the highest elongation and tensile strength among all specimens; while, the strength values of specimens 309L and 316L were close to each other (Fig. 10). Type 309L weld metal had the maximum amount of austenite in the microstructure which improved the elongation values. It is suggested that the solid solution strengthening phenomenon compensated for the minimum amount of delta ferrite in this weld; consequently, the tensile strength of the specimen was increased.

Furthermore, the tensile strength values of the longitudinal specimens were higher than that of the transverse ones. These findings confirmed the deleterious effect of the grain boundary martensite and grain growth phenomenon on the mechanical properties of the ferritic HAZ. Moreover, no evidence of harmful phases like martensite and chromium carbide was found in any weld metals.

It is observed that type 309L filler metal offered the better mechanical properties of the weld metal; while all transverse tension samples were fractured in the ferritic HAZ. On the other hand, type 2594 weld metal had the highest percentage of delta ferrite. Also, austenite and delta ferrite showed nearly the same chemical composition and hardness in this specimen. The presence of delta ferrite is necessary to avoid hot cracking, and the similar characterizations of austenite and ferrite can be useful in corrosive environments. However, more studies are needed to find the most corrosion resistant weld among these specimens. If the corrosion is not a concern, type 309L weld metal can provide the proper mechanical properties of the austenitic-ferritic dissimilar joints at a low price.

## 4. Conclusions

The gas tungsten arc welding was carried out on the ferritic-austenitic stainless steel joints. Type ER309L, ER316L and
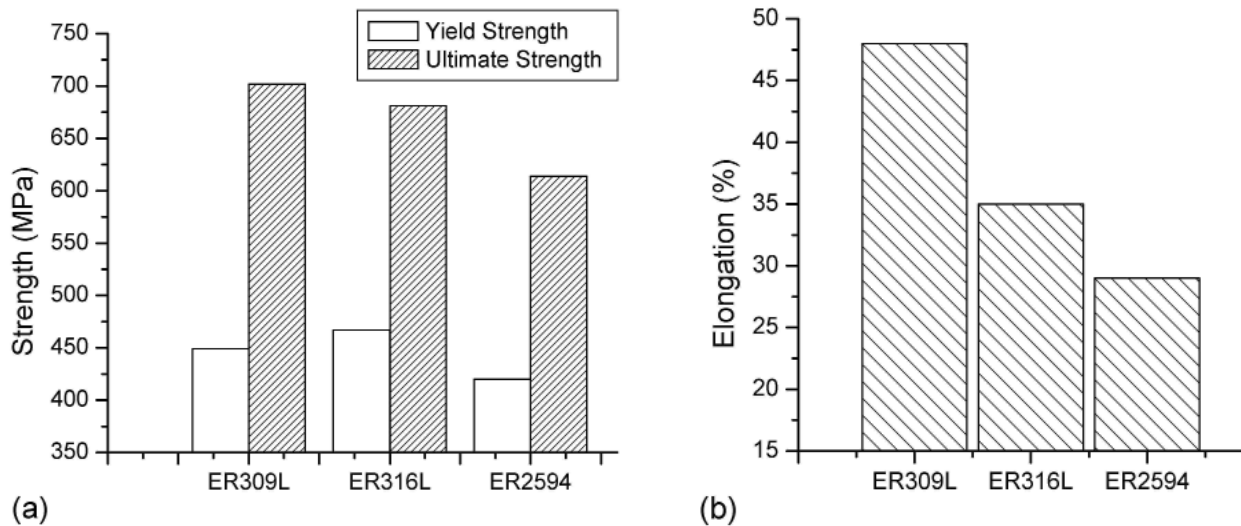
Fig. 10. The results of longitudinal tension tests: (a) Tensile and yield strength; (b) Elongation values

ER2594 filler metals were used in this study. The grain growth phenomenon was accompanied by the martensite formation in the HAZ of ferritic stainless steel; therefore, this region was the weakest zone in all specimens. The hardness and tensile strength of the weld metals were higher than that of the heat affected zones and the base metals. The chemical composition of delta ferrite and austenite in type 2594 joint was astonishingly similar and led to the same hardness values of these phases; while the ferrite presented higher hardness values than austenite in type 316L and 309L weld metals. Type 309L weldment showed the highest tensile strength among all specimens.

REFERENCES

[1]  T. Mohandas, M.G. Reddy, M. Naveed, J. Mater. Process. Technol. **94**, 133-140 (1999).

[2]  J.C. Lippold, D.J. Kotecki, Welding Metallurgy and Weldability of Stainless Steels, 2005 Wiley-Interscience, New Jersey, Hoboken.

[3]  F.B. Pickering, Int. Met. Rev. **21**, 227-268 (1976).

[4]  S. Kumar, A.S. Shahi, Mater. Design **32**, 3617-3623 (2011).

[5]  M. Shojaati, B. Beidokhti, Constr. Build. Mater. **147**, 608-615 (2017).

[6]  C.J. Long, W.T. Delong, Weld. J. **32**, 281s-297s (1973).

[7]  C.C. Hsieh, D.Y. Lin, M.C. Chen, W. Wu, Mater. Sci. Eng. A **477**, 328-333 (2008).

[8]  K. Shanmugam, A.K. Lakshminarayanan, V. Balasubramanian, Int. J. Mater. Sci. Technol. **25**, 181-186 (2009).

[9]  D.J. Kotecki, Weld. J. **84**, 14s-16s (2005).

[10]  M. Mukherjee, T.K. Pal, J. Mater. Sci. Technol. **28**, 343-352 (2012).

[11]  A.F. Padilha, C.F. Tavares, M.A. Martorano, Mater. Sci. Forum **730-732**, 733-738 (2013).

[12]  T. Maki, C.M. Wayman, Acta Metall. **25**, 681-693 (1977).

[13]  X.M. Zhang, E. Gautier, A. Simon, Acta Metall. **37**, 477-485 (1989).

[14]  E. Taban, E. Kaluc, A. Dhooge, Mater. Design **30**, 4236-4242 (2009).

[15]  T.D. Anderson, M.J. Perricone, J.N. Dupont, A.R. Marder, Weld. J. **86**, 281s-292s (2007).

[16]  J.A. Brooks, A. Thompson, Int. Mater. Rev. **36**, 16-44 (1991).

[17]  L. Li, R.W. Messler, Jr., Weld. J. **5**, 78s-84s (2002).

[18]  Y. Arata, F. Matsuda, H. Nakagawa, S. Katayama, Trans. JWRI **7**, 21-24 (1978).

[19]  J.A. Brooks, Weld. J. 54, 189s-195s (1975).

[20]  M. van Warmelo, D. Nolan, J. Norrish, Mater. Sci. Eng. A **464**, 157-169 (2007).

[21]  M.M.A. Khan, L. Romoli, M. Fiaschi, G. Dini, F. Sarri, J. Mater. Process. Technol. **212**, 856-867 (2012).

[22]  C.T. Kwok, S.L. Fong, F.T. Cheng, H.C. Man, J. Mater. Process. Technol. **176,** 168-178 (2006).

[23]  W. Reick, M. Pohl, A.F. Padilha, ISIJ Int. **38**, 567-571 (1998).

[24]  R.E. Avery, Pay Attention to Dissimilar-Metal Welds: Guidelines for Welding Dissimilar Metals, 1991, Nickel Development Institute, Toronto.

[25]  D.J. Lee, K.H. Jung, J.H. Sung, Y.H. Kim, K.H. Lee, J.U. Park, Y.T. Shin, H.W. Lee, Mater. Design **30**, 3269-3273 (2009).

[26]  U. Caligulu, H. Dikbas, M. Taskin, Gazi U. J. Sci. **25**, 35-51 (2012).

[27]  L.J. Ayers, The Hardening of Type 316L Stainless Steel Welds with Thermal Aging. B.Sc. Thesis, Massachusetts Institute of Technology, Massachusetts, 2012.

[28]  Y. Cao, Y.B. Wang, X.H. An, X.Z. Liao, M. Kawasaki, S.P. Ringer, T.G. Langdon, Y.T. Zhu, Acta Mater. **63**, 16-29 (2014).

[29]  C.J. Huang, D.J. Browne, S. McFadden, Acta Mater. **54**, 11-21 (2006).

[30]  T. Sakaki, K. Sugimoto, T. Fukuzato, Acta Metall. **31**, 1737-1746 (1983).

[31]  S.K. Paul, Mater. Design **50**, 782-789 (2013).